

multiplying the average sample weight during the test increment times equivalent distance traveled during the test increment, dividing the product by cycle duration in seconds, and normalizing the result by the area of the bottom 1/8 (45°) of the test drum where sample fragments reside during slake durability testing. The geotechnical scour number is equivalent scour depth divided by equivalent stream power. An example calculation is presented in Figure 5 for thinly bedded siltstone at the bridge on the Sacramento River in Redding, CA, USA, shown in Figure 4.

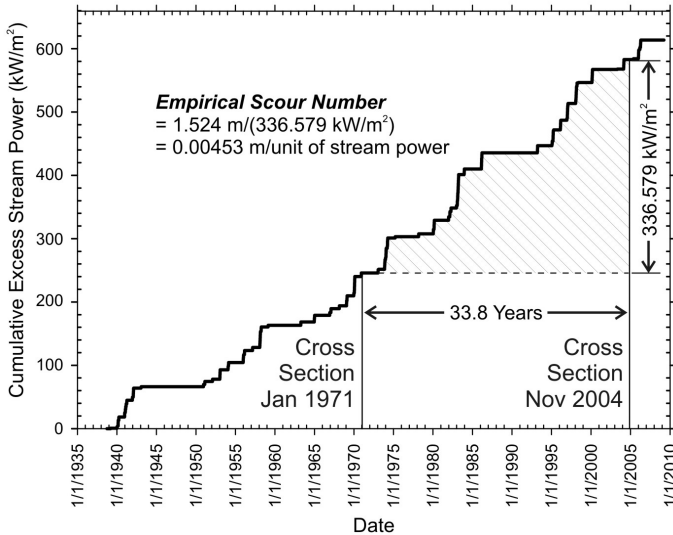


Figure 4. Empirical scour number calculation from daily stream power at the US Geological Survey Keswick gage on the Sacramento River at Redding produced by 2-year and larger discharge events. Cross sections on the upstream edge of a state highway bridge revealed 1.524 m (5 ft) of scour over 33.8 years.

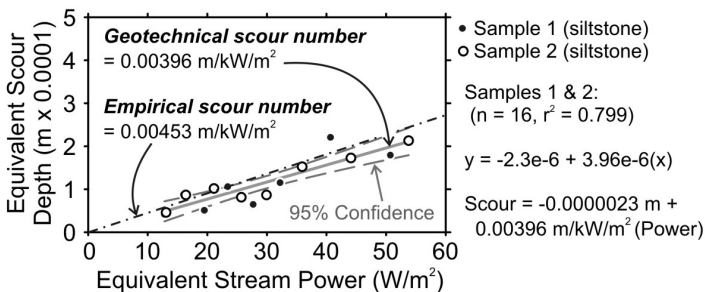


Figure 5. Geotechnical scour number calculation for siltstone samples from the bridge site in Figure 4. Empirical scour number from Figure 4 plotted for comparison.

SCOUR RATE AND DEPTH

The time-rate of scour is specific to different scour modes. Dissolution of soluble rocks in water occurs relatively slowly for rocks with suitable load-bearing capacity to support bridge structures. The scour rate of interest for soluble rocks would be governed by void-filling mixtures of rock fragments in a soil matrix too heterogeneous to be generalized. Scour rates in the soil matrix would govern the time-rate of scour. Rock blocks and fragments will collect in the scour hole if they are too large to be transported, thereby creating a natural armor condition on the channel bed and limiting the depth of scour.

Scour caused by threshold-controlled processes, such as cavitation or plucking, typically is assumed to develop to the maximum depth rapidly as soon as the threshold condition is exceeded. The depth of cavitation scour in natural channels has not been determined because cavitation is unstable and probably self-limiting by air entrainment and channel adjustments. The depth of plucking has been estimated by index methods (NRCS, 2001; Annandale, 2006) developed largely from empirical data collected in unlined spillway channels. Numerical modeling of threshold flow velocities for rock block plucking performed by Bollaert (5th ICSE) predicted scour depth relative to pier diameter; calibration of the model is needed for hydraulic conditions and geometries of natural channels.

Gradual and progressive scour of degradable rocks can be related to cumulative stream power and the empirical or geotechnical scour number. Flood frequency is calculated from daily flow series if gage data are available; otherwise, it can be estimated using conventional watershed relationships (Mishra et al., 5th ICSE). Flood event discharge is correlated to a cumulative excess stream power and then converted to scour depth by applying the empirical or geotechnical scour number. The inverse of flood return period is frequency; for example, the 2-year discharge corresponds to an average annual frequency of 0.5, whereas the 100-year discharge corresponds to an average annual frequency of 0.01. The area under the probability weighted flood frequency-scour depth curve is the average annual scour, as shown in Figure 6. The examples in Figure 6 consist of the Sacramento River at Redding, Shasta County, CA, and Schoharie Creek at the Interstate Highway 90 crossing in Montgomery County, NY. Shasta Dam on the Sacramento River was closed in 1945 and the discharge has been regulated since that time. Schoharie Creek is an unregulated watershed draining the north side of the Catskill Mountains.

Design scour depth is the product of the probability weighted average annual scour and the remaining life of a bridge structure or the product of cumulative stream power for the life of a bridge and the appropriate scour number. The amount of pier scour at the State Route 273 Bridge on the Sacramento River documented by California Department of Transportation over a 33.8-year period was 1.524 m (5 ft); the amount of scour calculated from the average annual scour at this location is 1.6 m ($33.8 \text{ yr} \times 0.048 \text{ m/yr}$ from Figure 6). The amount of pier scour at the Interstate 90 Bridge on Schoharie Creek determined from forensic studies of the 1987 bridge failure (Resource Consultants and Colorado State University, 1987) was about 4.6 m (15 ft); the amount of scour calculated from the average annual scour at this bridge is 5.1 m ($33 \text{ yr} \times 0.155 \text{ m/yr}$ from Figure 6).

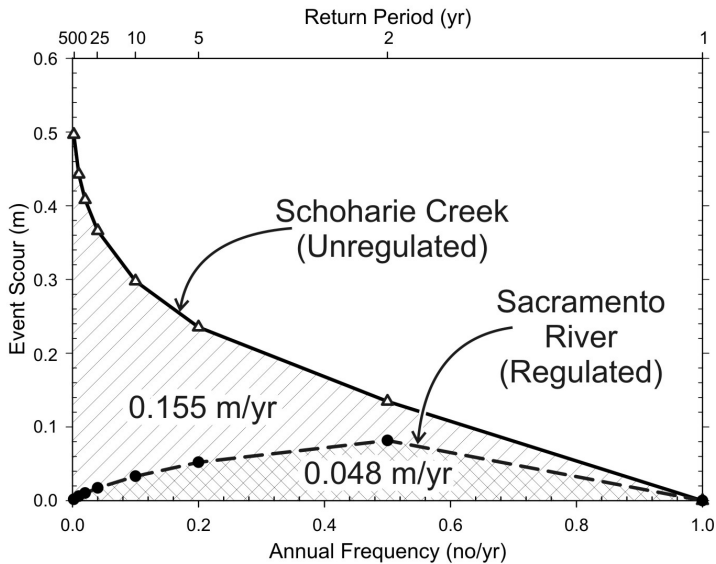


Figure 6. Probability weighted average annual scour for the Sacramento River, CA, and Schoharie Creek, NY. Sacramento River is regulated by Shasta Dam.

DISCUSSION AND CONCLUSIONS

Rock scour is a rock-water interaction phenomenon. Rock material ranges in properties from slightly better than good soil to much better than the best concrete. No rock material is resistant to the forces of water in the form of waterjets used to strip concrete away from reinforcing steel for bridge deck rehabilitation (Summers, 1995). In fact, waterjets can cut through the reinforcing steel if they are applied long enough. In natural, open channels, however, the stream power tends to be low enough that most rock materials can resist the hydraulic forces to some degree.

Soluble rock dissolution is not likely to be an important process at bridge sites because rocks that dissolve in engineering time have poor load-bearing capacity and would not be used for bridge support. Cavitation is not likely to be an important process at bridge sites because most natural channels cannot support the required hydraulic conditions or such channels would be spanned by bridges.

Durable rock plucking is analogous to scour of giant, interlocking sand grains. Threshold conditions characterized by hydraulic parameters at peak discharge control rock-block plucking similar to sand grains on sand-bed channels. Scour holes in sand-bed channels are thought to form rapidly as threshold conditions are reached; the holes are backfilled during waning stages of discharge with sand similar in character to the initial bed. Scour holes in rock-bed channels may be backfilled, but such backfill would not have the resistance of the initial rock-bed channel.

Degradable rock scour is gradual and cumulative. Threshold conditions probably exist, but scour holes develop in response to the applied hydraulic forces. The 100-year discharge may cause scour at a higher rate than the 2-year discharge,

but if the 100-year discharge duration is very small compared to the 2-year discharge duration, then the overall contribution to scour by the 100-year discharge would be much less than the 2-year discharge. The probability weighted average annual scour captures this concept. Index methods (NRCS, 2001; Annandale, 2006) applied to Sacramento River conditions show that the hydraulic loading is less than the scour resistance of the siltstone even though 1.5 m of scour has been documented.

REFERENCES

- Annandale, G.W. (2006). *Scour Technology*, New York, McGraw-Hill, 430 p.
- Baker, V.R., and Costa, J.E. (1987). Flood Power, in Mayer, L., and Nash, D., eds., *Catastrophic Flooding*, Boston, Allen & Unwin, p. 1-21.
- Barnes, H.L. (1956). Cavitation as a Geological Agent *American Journal of Science*. v. 254, p. 493-505.
- Bollaert, E.F.R. (2010). Numerical Modelling of Scour at Bridge Foundations of Rock, *Proceedings 5th International Conference on Scour and Erosion* (this conference).
- Hancock, G.S., Anderson, R.S., and Whipple, K.X. (1998). Beyond Power: Bedrock Incision Process and Form, in Tinkler, K.J., and Wohl, E.E., eds., *Rivers Over Rock: Fluvial Processes in Bedrock Channels*, American Geophysical Union, Geophysical Monograph 107, p. 35-60.
- Keaton, J.R., and Mishra, S.K. (2010). Modified Slake Durability Test for Erodible Rock Material, *Proceedings 5th International Conference on Scour and Erosion* (this conference).
- Mishra, S.K., Keaton, J.R., Clopper, P.E., and Lagasse, P.F. (2010). Hydraulic Loading for Bridges Founded on Erodible Rock, *Proceedings 5th International Conference on Scour and Erosion* (this conference).
- NRCS (2001). Field Procedures Guide for the Headcut Erodibility Index: Chapter 52, Part 628, *National Engineering Handbook*, U.S. Department of Agriculture Natural Resources Conservation Service, 210-VI-NEH, revol. 1, March, 37 p
- Reinius, E. (1986). Rock Erosion, *Water Power & Dam Construction*, v. 38, p. 43-48.
- Resource Consultants, Inc. and Colorado State University (1987). *Hydraulic, Erosion, and Channel Stability Analysis of the Schoharie Creek Bridge Failure*, New York, Consulting report prepared for National Transportation Safety Board and New York State Thruway Authority, paginated by section.
- Richardson, E.V., and Davis, S.R. (2001). Evaluating Scour at Bridges. Hydrologic Engineering *Circular 18*, Federal Highway Administration, 4th Edition, Publication No. NHI 01-001, 378 p.
- Summers, D.A. (1995). *Waterjetting Technology*, London, E & FN Spon, 616 p.
- Tinkler, K.J., and Parish, J. (1998). Recent Adjustments to the Long Profile of Cooksville Creek, and Urbanized Bedrock Channel in Mississauga, Ontario, in Tinkler, K.J., and Wohl, E.E., eds., *Rivers Over Rock: Fluvial Processes in Bedrock Channels*, American Geophysical Union, Geophysical Monograph 107, p. 167-187.
- Whipple, K.X., Hancock, G.S., and Anderson, R.S. (2000). River incision into bedrock: Mechanics and relative efficacy of plucking, abrasion, and cavitation *Geological Society of America Bulletin*. v. 112, no. 3, p. 490-503.

Bluestone Dam Rock Scour

M. F. George¹, PE and G.W. Annandale², D.Ing, PE, D.WRE

¹Project Geological Engineer, Golder Associates Inc., Lakewood, CO 80227; PH: 303-980-0540; email: Michael_George@Golder.com

²Practice / Program Leader, Golder Associates Inc., Lakewood, CO 80227; PH: 303-980-0540; email: George_Annandale@Golder.com

ABSTRACT

Advancements in hydrologic methods have often yielded greater estimates for design flood events. This can be problematic for older dams when the constructed spillway can no longer adequately pass the revised flood estimate. Bluestone Dam is one such case where recent estimates have indicated more than a twofold increase in the design flood magnitude. Moveable bed physical hydraulic model studies for flows greater than the original design indicated complex flow conditions and the potential for significant scour in the unlined hydraulic jump stilling basin. The ability of the homogeneous gravel used in the model study to represent scour potential of intact rock in the actual basin was questionable. As such, Annandale's Erodibility Index Method was used to provide revised scour estimates within the stilling basin. This paper presents a unique solution to a complex problem.

Introduction & Background

Bluestone Dam is a concrete gravity dam located on the New River near Hinton, WV (USA). Built during the 1940's, the dam has a 241 m long spillway with 21 gated overflow spillway bays and 16 lower sluice gates. Flow from the spillway discharges into an unlined hydraulic jump stilling basin (Figure 1). A downstream weir controls the water level within the stilling basin, while baffles on the stilling basin apron and an end sill at the end of the apron are provided to dissipate energy and direct flow upwards before entering the basin. The dam also has six large penstocks (~ 6 m diameter) that can be opened to provide additional discharge capacity.

The spillway was originally designed to pass a probable maximum flood (PMF) event of 12,180 m³/s while recent advancements in hydrologic methods, however, have indicated more than a twofold increase in the design flood magnitude to 28,320 m³/s.

Local geology within the stilling basin consists of three main rock types: orthoquartzite, interbedded shale and orthoquartzite, and claystone.



Figure 1. Bluestone Dam layout (Photo courtesy of USACE – Huntington District, Engineering Geology Section).

Physical Hydraulic Model Study

A 1:36 scale physical hydraulic model study was performed to examine scour potential from increased flows beyond the original design discharge up to the revised PMF of $28,320 \text{ m}^3/\text{s}$ (USACE 2003b). A homogenous gravel bed, consisting of 1 cm size particles, was used to represent rock within the stilling basin.

Based on observation of the video taken of the physical hydraulic model, two main flow conditions exist over the range of discharges analyzed. For discharges up to the original design discharge, the basin functions as designed and a relatively well formed hydraulic jump is witnessed with little to no scour occurring. For the larger discharges, however, flow exiting the spillway into the basin closely resembles that of a “shooting jet”. Comparison of the two scenarios is shown in Figure 2.

For the latter scenario, the end sill on the stilling basin apron directs flow upwards (similar to that of a flip bucket), causing the jet to skim on top of the tailwater in the basin and plunge downwards upon impact with the upstream face of the stilling basin weir. Scour-hole formation occurs on the upstream side of the stilling basin weir. Tailwater within the stilling basin is re-circulated forming a large eddy that transports scoured material in the downstream portion of the basin back towards the apron.

Results from the 1:36 scale model indicate a potential for up to 27 m of scour within the basin under the revised PMF conditions, which would undoubtedly result in failure of the stilling basin weir. As using gravel to evaluate scour of intact rock in physical model studies may not be representative, it was desirable to attempt to determine how actual rock in the basin would influence scour.

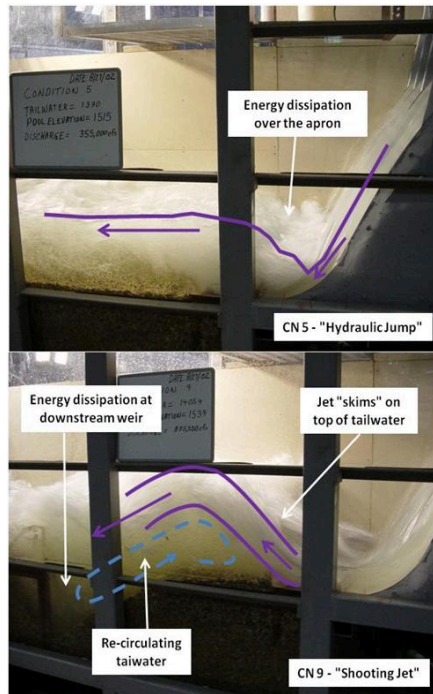


Figure 2. Comparison of flow conditions for discharges less than (top) and greater than (bottom) the original design discharge. Photos courtesy of USACE – Huntington District.

Calibration of Erosive Capacity

For discharges above the original design, flow conditions within the stilling basin are unique, and no one methodology can perfectly represent these conditions. As indicated in Figure 2, higher discharges loosely resemble a shooting jet and therefore jet and plunge pool theories were applied in an attempt to model these distinctive hydraulic conditions with known methods. Figure 3 shows a cross-section of the dam and stilling basin with a schematic of the plunging jet scour module as applied to Bluestone.

The methodology was modified by use of a calibration factor, applied to the calculation of flow erosive capacity within the stilling basin, to account for inadequacies of directly applying the plunging jet module to this flow scenario. Specifically this was done to account for 1) energy dissipation associated with flow through the baffle blocks on the basin apron, 2) the reduction in the jet flow rate applied to the stilling basin floor as an unknown portion of the jet is directed over the stilling basin weir, and 3) energy dissipation associated with jet impinging against the

back of the stilling basin weir and being re-directed downwards. The calibration factor was determined through the aid of the 1:36 scale physical hydraulic model.

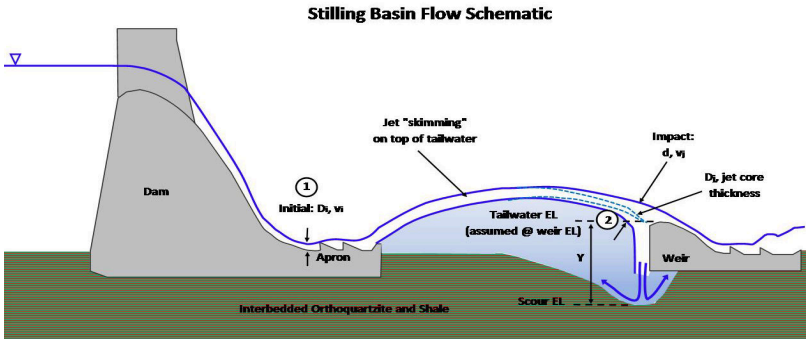


Figure 3. Schematic for shooting jet scenario showing applied plunge pool module (schematic based on typical section from USACE (2003a)).

For theoretical scour predictions, the erosive capacity of the plunging jet (expressed in units of stream power, W/m^2) could be calculated using Annandale's Erodibility Index Method (EIM) (1995, 2006):

$$P_{jet} = \frac{\gamma \cdot Q \cdot H}{A \cdot K} \cdot C_t$$

Where:

γ = unit weight of water (N/m^3).

Q = water discharge (m^3/s).

H = hydraulic head associated with the falling jet (m) taken between locations "1" and "2" on Figure 3.

A = impact area of the jet (i.e., jet footprint) (m^2).

K = factor to calibrate calculated erosive capacity to observed erosive capacity witnessed in the model study (see discussion below).

C_t = total dynamic pressure coefficient (dimensionless) used to determine the relative magnitude of erosive capacity as a function of tailwater depth. Although derived from pressure measurements, use of C_t to portray trends in erosive capacity within the plunge pool quantified by stream power has shown good promise (see George & Annandale 2006a, 2006b, 2008 and Lund et al. 2008). C_t can be expressed as:

$$C_t = C_p + RF \cdot \Gamma \cdot C_p^2$$

Where:

C_p = average dynamic pressure coefficient as a function of tailwater depth based on work by Castillo et al. (2007).

Γ = amplification factor to account for resonance that may occur in close-ended rock fissures as a function of tailwater depth (Bollaert 2002). Note that $\Gamma = 1$ (i.e., no amplification) for the calibration with physical model results (as the bed material is gravel) as well as for the theoretical scour calculations as characteristic frequencies for orthoquartzite and shale rock fissures were found not to be within the frequency range of major pressure fluctuations.

RF = unit reduction factor to account for influence of varying degrees of jet break-up based on work by Ervine et al. (1997).

C'_p = fluctuating dynamic pressure coefficient as a function of tailwater depth based on work by Bollaert (2002).

To calibrate the calculated erosive capacity with the erosive capacity observed in the 1:36 scale physical hydraulic model, the calibration factor, K , was adjusted such that the theoretical scour depth matched the observed scour depth in model (Figure 4). Doing so required knowledge of the prototype erosion resistance of the gravel used in the physical model. This is discussed in the following section.

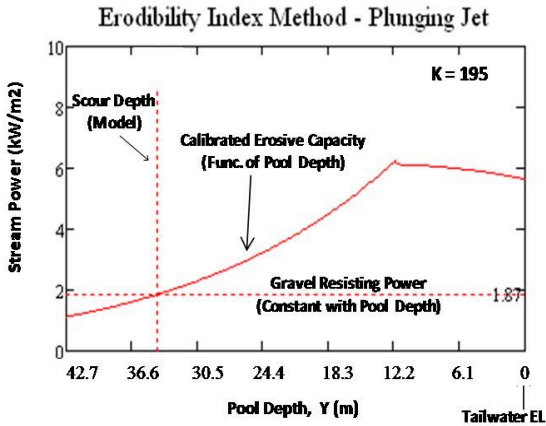


Figure 4. Example of erosive capacity calibration for revised PMF discharge.

Material Resistance

For the calibration, the erosion resistance provided by the gravel in the physical model study could be determined from the critical shear resistance calculated using the Shields parameter (1936) for cohesionless materials.

$$\tau_c = \theta_c \cdot (\rho_s - \rho) \cdot g \cdot d$$

Where:

θ_c = critical Shields parameter for rough turbulent flow = 0.06 (dimensionless).

ρ_s = particle density (kg/m^3).

ρ = water density (kg/m^3).

g = acceleration due to gravity (m/s^2).

d = diameter of gravel used in physical model = 0.01 m.

Using the scale law for stream power between model and prototype, the prototype resisting power of the gravel could be calculated using the following equation from Annandale (2006):

$$P_{cp} = 7.853 \cdot \rho \cdot \left(\sqrt{\frac{\tau_c}{\rho}} \right)^3 \cdot L_s^{\frac{3}{2}}$$

Where:

L_s = model scale = 36 (dimensionless). This value is raised to an exponent of three-halves to convert from model resisting power to prototype resisting power.

Once the calculated erosive capacity has been calibrated with the model scour results (based on the prototype resisting power of the gravel), the actual rock resistance can be inserted into the plunge pool scour module to determine a revised estimate for scour depth. Rock erodibility can be determined using the EIM (Annandale, 1995): The erodibility index, K_{hs} , can be defined as:

$$K_h = M_s \cdot K_b \cdot K_d \cdot J_s$$

Where:

M_s = mass strength number.

K_b = block/particle size number. For rock, $K_b = \text{RQD}/J_n$, where RQD is the rock quality designation and J_n is the joint set number.

K_d = discontinuity/interparticle bond shear strength number. For rock, $K_d = J_r/J_a$, where J_r is the joint roughness number and J_a is the joint alteration number.

J_s = relative ground structure number.